

Optically detected cyclotron resonance of GaAs quantum wells: Effective-mass measurements and offset effects

R. J. Warburton, J. G. Michels, and R. J. Nicholas

Clarendon Laboratory, Parks Road, Oxford, OX1 3PU, United Kingdom

J. J. Harris

*Semiconductor Interdisciplinary Research Centre, Imperial College of Science and Technology,
Blackett Laboratory, Prince Consort Road, London, United Kingdom*

C. T. Foxon

Physics Department, Nottingham University, Nottingham, United Kingdom

(Received 16 July 1992)

We have detected cyclotron resonance in a series of undoped GaAs quantum wells by modulating the photoluminescence intensity with far-infrared radiation. The conduction-band mass was measured for different quantum-well widths, and good agreement with a simple formula based on $\mathbf{k} \cdot \mathbf{p}$ theory is achieved. An offset was observed in the cyclotron-resonance energy, strongly dependent on well width. The interpretation is that monolayer-width fluctuations localize the carriers, giving an additional binding energy to the cyclotron-resonance transition.

I. INTRODUCTION

In optically detected cyclotron resonance (ODCR), resonant absorption of long-wavelength radiation is detected through its effects on the photoluminescence intensity. It has been recently shown that the power output of a far-infrared laser is sufficient to give large ODCR signals in bulk semiconductors.^{1,2} This allows measurements in high magnetic fields to be made. Although the ODCR mechanisms are not that well understood, it is now clear experimentally that the ODCR technique can be much more sensitive than straightforward absorption experiments.^{3,4} Furthermore, ODCR allows cyclotron-resonance measurements to be made on undoped material, and also it is hoped that it will be possible, in the far infrared, to optically detect both electron and hole resonances in the same sample.

In this paper, we report ODCR measurements on a series of GaAs quantum wells. The conduction-band mass was measured as a function of well width, and the data agree well with a simple formula based on $\mathbf{k} \cdot \mathbf{p}$ theory, as derived by Ekenberg.⁵ A further result concerns an offset in the cyclotron-resonance energies. The offset is the cyclotron-resonance energy when the magnetic field is extrapolated to zero. We find that the offset is strongly dependent on well width, scaling as $d\epsilon/dL$ where ϵ is the electron confinement energy and L the quantum-well width. We explain how this shows that the offset is caused by the localization of electrons by monolayer width fluctuations.

The advantage of the ODCR technique for this experiment is that we could use undoped samples. This allows the effective mass to be compared to *flat band* calculations, and makes the interpretation of the offset effect unambiguous. For doped samples, band bending must

be taken into account, and the interpretation of the offset effect is confused in this case because the potential from the ionized donors can also localize electrons in the quantum limit.

ODCR from two GaAs quantum wells has been previously reported by Ahmed *et al.*⁴ However, these authors used only a single cyclotron energy, and so did not observe an offset effect, which we report here.

II. EXPERIMENTAL DETAILS

ODCR requires two light sources: one in the near-infrared or visible region (to excite the luminescence), and one in the far-infrared or microwave region. In our case, we used a 3-mW solid-state laser diode operating at 670 nm, and an optically pumped molecular gas laser for the far infrared. All measurements were made with the sample at ~ 2.2 K in an 18-T superconducting magnet.

The 670-nm radiation arrived at the sample by means of one arm of a bifurcated fiber bundle; the second arm was used to collect the luminescence. The power density at the sample was ~ 5 mW cm⁻², which gives an estimated carrier density in each quantum well of $< 10^6$ cm⁻². This is very small compared to typical doping concentrations of $\sim 10^{11}$ cm⁻². The luminescence was dispersed with a 0.5-m spectrometer, and detected with a GaAs photomultiplier tube.

The far-infrared radiation travelled through a light pipe and then through two 45° reflections underneath the sample, so that the far infrared was incident on the sample substrate. The throughput of the far infrared was continuously monitored with a bolometer placed next to the fiber bundle. We used about ten methanol (or deuterated methanol) far-infrared lines, with wavelengths between ~ 300 and 70 μm .

TABLE I. The well widths, measured masses, measured confinement energies, and the calculated masses. The calculated masses come from Eq. (2) using $m_0^* = 0.0665$ and the measured confinement energies.

Sample	G50	G57	G51	G55
Width ^a (Å)	25.7	56	73.4	112.5
Measured m^* ($\times 10^{-3} m_e$)	81.8 ^b	78.1	74.3	70.8
Measured ε (meV)	198 ^c	78	50	29
m^* from measured ε ($\times 10^{-3} m_e$)		76.8	73.1	70.3

^aX-ray measurements (Ref. 6).

^bReference 9.

^cReference 7.

The samples for the experiment were high quality GaAs quantum wells, grown at Philips, Redhill. Each is a multi-quantum well, consisting of 60 nominally identical GaAs/Al_{0.36}Ga_{0.64}As wells. Extensive characterization details can be found in Orton *et al.*⁶ The sample well widths are listed in Table I. The samples have been previously used for interband magneto-optic experiments^{7,8} which confirm that they are of high quality. Also, the 25.7-Å sample was used in a pump-probe experiment,⁹ in which electrons were excited with a red light-emitting diode, and cyclotron resonance detected by far-infrared photoconductivity.

III. RESULTS

Figure 1 shows the photoluminescence and the ODCR signals as a function of detection energy for the 56-

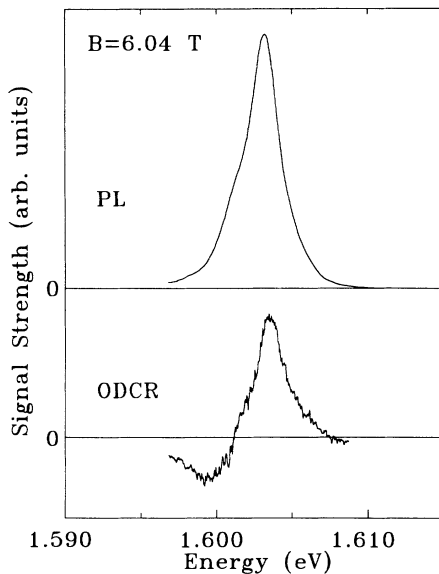


FIG. 1. Photoluminescence (PL) and optically detected cyclotron-resonance (ODCR) signals vs detection energy for sample G57, a 56-Å GaAs/Al_{0.36}Ga_{0.64}As quantum well. The ODCR was carried out with far-infrared wavelength 118.8 μm . The field, 6.04 T, is the field for electron cyclotron resonance.

Å quantum well at the resonance field. The ODCR spectrum roughly follows the derivative of the photoluminescence spectrum. The overall ODCR response, integrated over energy, is positive (i.e., the far-infrared increases the photoluminescence intensity). Curves similar to Fig. 1 were obtained away from resonance, but with a smaller ODCR signal. The form of ODCR in Fig. 1 could be caused by carrier heating, or some form of carrier delocalization, both of which could enhance the photoluminescence on the high-energy side of the peak. The integrated ODCR signal was at best +1.0% with our strongest laser line, 118.8 μm . Most of our data were taken with fairly wide spectrometer slits, with resolution comparable to the diamagnetic shift of the luminescence peak at high magnetic field, so that we did not need to continually adjust the detection wavelength when sweeping the field. Such an ODCR trace is shown in Fig. 2 from sample G51, taken with the 118.8- μm far-infrared line. The prominent peak is the electron cyclotron resonance. The peak is fairly broad (half width 0.3 T) and this is largely caused by well-to-well fluctuations in the well width. Figure 2 shows also that the background response, which is quite large at zero field, decays rapidly in the first few tesla, but returns at high field to approximately the zero field level. The background was less noticeable at wavelengths longer than $\sim 150 \mu\text{m}$. Unfortunately, we could not observe any cyclotron resonances from sample G50, the 25.7-Å well sample. An ODCR signal was observed only for short wavelengths (e.g., 70.5 μm), but it consisted of only the background response without any resonant features. It is not clear why this should be, as the 25.7-Å sample is certainly of high quality. Experimentally, our results are consistent with those of Ahmed *et al.*⁴ who could also find no

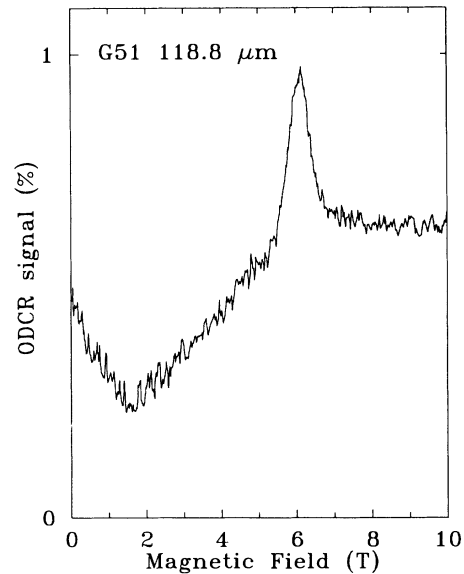


FIG. 2. Integrated ODCR signal vs magnetic field for sample G51, a 73.4-Å quantum well, with far-infrared wavelength 118.8 μm . The prominent peak is the electron cyclotron resonance.

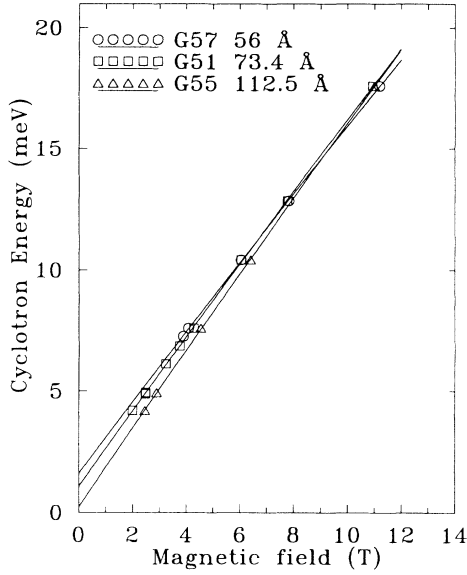


FIG. 3. The data collected by ODCR at several far-infrared wavelengths for the quantum-well samples, plotted as cyclotron energy vs magnetic field. The plot shows how the low field slope decreases and the offset (the cyclotron energy extrapolated to zero field) increases as the well width decreases.

ODCR from narrow GaAs quantum wells. It is curious that the pump-probe experiment of Singleton *et al.*⁹ was only successful for the 25.7-Å quantum well and not for the wider wells, so the two techniques, pump-probe and ODCR, are apparently complementary for these samples.

Cyclotron-resonance data for samples G57, G51, and G55 are collected together in Fig. 3, a plot of the cyclotron energy, E_{CR} , against magnetic field, B . The data were fitted to

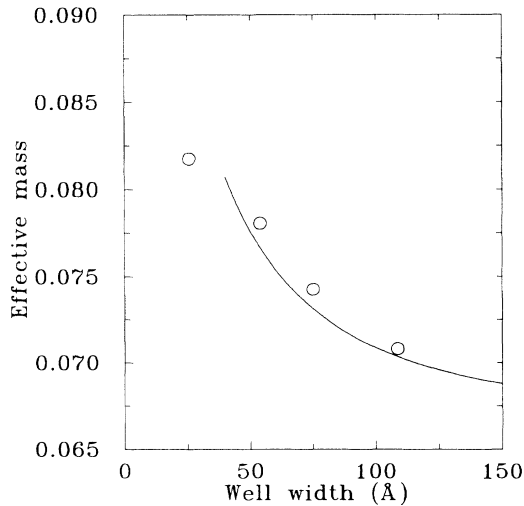


FIG. 4. Effective mass (in units of the free-electron mass) vs quantum-well width. The solid line is the theory of Ekenberg, as discussed in the text.

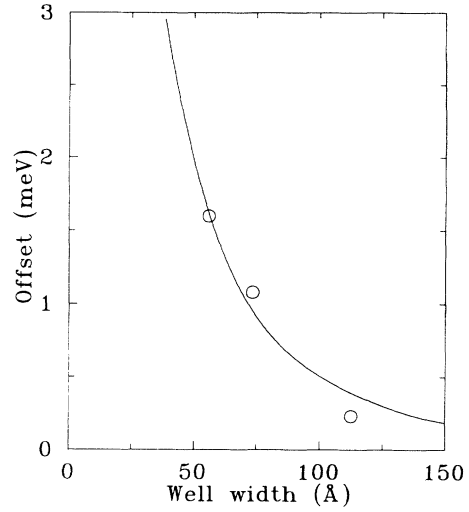


FIG. 5. Cyclotron-resonance offset energy vs quantum-well width. The solid line is Eq. (10) with $\gamma = \frac{1}{3}$.

$$E_{CR} = E_o + E_1 B + E_2 B^2. \quad (1)$$

E_1 determines the slope at low field, and hence the band edge mass of the quantum well, $m^* = e\hbar/E_1$. Figure 3 shows how the slope decreases, and hence the mass increases, with decreasing well width. The explanation is that as the well width decreases, the confinement energy increases, giving a larger nonparabolicity correction to the bulk GaAs mass. The term E_2 in Eq. (1) arises from nonparabolicity in the quantum-well in-plane dispersion relation. To within our experimental error, E_2 was the same for the three samples. The energy E_o is the offset energy. Figure 3 shows clearly how the offset increases for decreasing well width.

The dependence on well width of the effective mass and offset energy are plotted in Figs. 4 and 5. Figure 4 contains also the band edge mass of the 25.7-Å sample as deduced from the pump-probe experiment. Note that with these samples it is essential to take into account the offset energy to reliably determine the effective mass. If the mass were deduced simply from $m^* = e\hbar B/E_{CR}$ then large errors would arise. For instance, Fig. 3 shows that if the masses were measured only, say, with $E_{CR} = 7.6$ meV (163 μm), then one would conclude that the mass decreases with decreasing well width.

IV. THE EFFECTIVE MASS

To calculate the effective mass as a function of well width, the confinement energy must be evaluated, and then from this the nonparabolicity enhancement to the bulk GaAs mass, m_0^* . Band nonparabolicity arises from interaction of the Γ_1^c conduction band with the Γ_5^v valence band and with the higher Γ_5^c conduction band. Rössler¹⁰ has shown that the Γ_1^c - Γ_5^c interaction must be included for energies more than ~ 50 meV above the band edge. This is the energy range here, because the confinement energy

is ~ 80 meV for the 57-Å quantum well. Ekenberg⁵ has considered both sources of band nonparabolicity and derived that for an infinitely deep well, to first order in the confinement energy ε ,

$$m^* = m_0^* [1 + (2\alpha' + \beta')\varepsilon] \quad (2)$$

where $\alpha' = -(2m_0^*/\hbar^2)^2\alpha_0$, $\beta' = -(2m_0^*/\hbar^2)^2\beta_0$, with α_0 and β_0 band parameters from Rössler.¹⁰ Numerically for GaAs,^{5,11} $\alpha' = 0.64$ eV⁻¹ and $\beta' = 0.70$ eV⁻¹, so that, for ε in eV,

$$m^* = m_0^* [1 + 1.98\varepsilon]. \quad (3)$$

Ekenberg⁵ showed also that in the case of a finite well, Eq. (2) still applies, providing that the penetration of the wave function into the barriers is small. Numerically, Eq. (2) works well for a 50-Å GaAs/Al_{0.3}Ga_{0.7}As quantum well compared to a theory that also includes the effects of the boundary conditions at the interfaces.⁵

To test Eq. (2) we have also measured the confinement energies ε . This eliminates any errors in the calculation of ε which would arise through uncertainties in the actual well widths. There are also problems in the effective-mass approach, in that there is no unique choice for the envelope function boundary conditions, and different choices can give significantly different results. For instance, Ekenberg⁵ considered three different boundary conditions, which, for a 50-Å well, give confinement energies differing by as much as 14 meV in a confinement energy of ~ 75 meV. The confinement energies ε were evaluated from the photoluminescence peak position E_{PL} , the exciton binding energy E_B , the GaAs band gap E_g ($=1.519$ eV), and the heavy-hole confinement energy E_{HH} :

$$\varepsilon = E_{PL} + E_B - E_g - E_{HH}. \quad (4)$$

E_{PL} was measured in our experiment; E_B is known from photoluminescence experiments by Moore, Dawson, and Foxon¹² on these samples, E_B being deduced from an observation of $2s$ exciton recombination; and E_{HH} was calculated using the x-ray widths.⁶ ε is determined to about ± 3 meV error. The values of ε are listed in Table I, and from these values we have calculated the masses from Eq. (2), also listed in Table I. The calculated masses can be compared with the experimentally measured points in Table I, and in Fig. 6, a plot of m^* versus ε . The theory can be seen to give a good fit to the experimental data.

Figure 6 shows that we have a linear variation of m^* with ε , but with a gradient slightly steeper than Eq. (2) predicts. The residual discrepancy could be caused by a number of factors, such as the omission of polaron enhancements in the theory, an error in the GaAs nonparabolicity at rather high energies above the band edge, or some additional error in the experimental data points. The polaron effect is known to be stronger in an ideal two-dimensional system than in an equivalent three-dimensional system,¹³ but this is not obvious in experiments on quasi-two-dimensional GaAs because of penetration of the wave function in the third dimension (and by screening in doped samples). A strong dimensionality

dependence, i.e., a ε dependence of the polaron enhancement is therefore not expected. In an attempt to model our data including both band and polaron nonparabolicity, we therefore extrapolate the cyclotron-resonance results of Hopkins *et al.*¹⁴ on bulk GaAs. These authors fitted the effective masses at low E_{CR} to

$$\frac{1}{m^*} = \frac{1}{m_0^*} \left[1 + \frac{2K_2}{E_g} E_{CR} \right], \quad (5)$$

with $K_2 = -1.75$ (an average of the two spin-split transitions). Replacing E_{CR} with ε , and inverting Eq. (5), we have

$$m^* = m_0^* [1 + 2.30\varepsilon]. \quad (6)$$

Figure 6 also includes this expression for the mass, and fits the data very well.¹⁵ For GaAs heterojunctions, Hopkins *et al.*¹⁶ used Eq. (5) but found $K_2 = -1.4$, reduced in magnitude from the bulk value because occupancy of the lowest Landau level prevents the polaron coupling process. $K_2 = -1.4$ implies $-2K_2/E_g \simeq 1.8$ eV⁻¹, which is essentially the same as Eq. (2), the difference being caused by the isotropic conduction band used in the derivation of Eq. (5). For the present case, the carrier concentration is so low that the polaron is not screened. It is likely then that the small discrepancy with Ekenberg's theory in Fig. 6 is caused by the polaron effect.

Figure 4 is a plot of m^* versus quantum-well width L . The solid line shows Eq. (2) using ε calculated with the three-band Kane model,¹⁷ with the boundary condi-

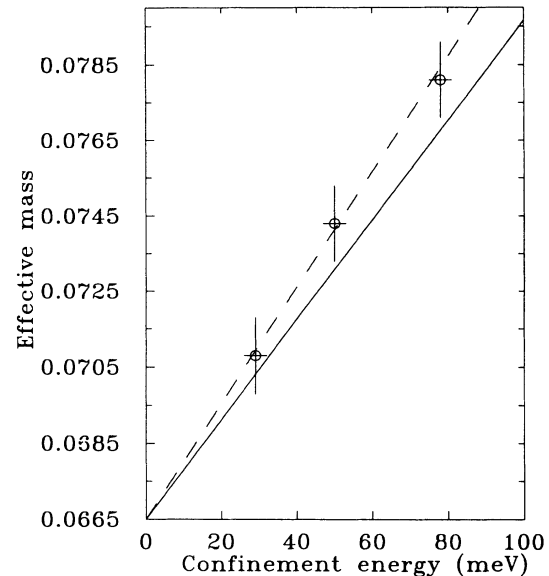


FIG. 6. A plot of measured effective mass vs measured electron confinement energy for the 56-, 73.4-, and 112.5-Å quantum wells. The data are modeled according to $m^* = m_0^* [1 + k\varepsilon]$ with $k = 1.98$ eV⁻¹ (solid line) from the theory of Ekenberg [Ref. 5 and Eq. (2)], and with $k = 2.30$ eV⁻¹ (dashed line) from the cyclotron-resonance results on bulk GaAs of Hopkins *et al.* [Ref. 14 and Eq. (5)].

tions of Bastard.¹⁸ The L 's of the data points plotted in Fig. 4 have been adjusted from their x-ray values such that the Kane model reproduces the measured confinement energies. No more than a one monolayer adjustment was necessary. Thus, for wells where Eq. (2) applies $[(2\alpha' + \beta')\varepsilon \ll 1]$, we can conclude that Eq. (2) successfully relates the parallel mass and the confinement energy. For the 25.7-Å sample, $(2\alpha' + \beta')\varepsilon \simeq 0.4$, which is no longer small compared to 1, and so Eq. (2) is no longer valid. However, Ekenberg⁵ considered this sample as a special case and calculated $\varepsilon = 205$ meV and $m^* = 0.080$, including the effects of the boundary conditions. These numbers agree well with the measured values of $\varepsilon = 198$ meV and $m^* = 0.082$, although this may be fortuitous given the absence of any polaron enhancement in the theory, and given the experimental uncertainty in the well width.

Finally, we note that it is important to include the nonparabolicity from the Γ_1^c - Γ_5^c interaction to model our results. Neglecting this coupling, by putting $K_2 = -1$ in Eq. (5), considerably underestimates the measured masses.

V. THE OFFSET

Offset effects have been observed and studied in ordinary cyclotron resonance with doped samples.^{19–23} The offset energy tends not to arise until the quantum limit is reached, when the electrons (or holes²³) condense into the localized states of the $n = 0$ level, and it is this extra localization energy that gives rise to the offset. At lower field more than one Landau level is occupied, and so the effect of the localizing potential is averaged out. Two models have been presented to analyze the offset energy. The first is that the observed cyclotron energy E_{CR} is perturbed from the intrinsic value E_{CR}^0 by a constant term:

$$E_{CR} = E_{CR}^0 + \delta, \quad (7)$$

as for the binding energy of a shallow impurity. Alternatively, one may suppose that the carriers are bound into a parabolic potential within the layers. For a one-dimensional potential $V(x) = \frac{1}{2}m^*(\delta/\hbar)^2x^2$ (with the growth direction z) one finds²⁴ that

$$(E_{CR})^2 = (E_{CR}^0)^2 + \delta^2. \quad (8)$$

The potential that causes this localization phenomenon can arise from several sources; for instance, the random potential from ionized donors, alloy disorder effects, or monolayer interface fluctuations. The potential need not be particularly large, and so can arise even in ultrahigh mobility heterojunctions.²²

In the present case, the density of electrons is very small and so we are in the quantum limit for all fields at which a resonance was recorded. The samples are of high quality and are nominally undoped, so there is no ionized donor potential to localize the carriers. The electron concentration is so low that it might be possible for each electron to bind onto a residual impurity in the wells. However, this is very unlikely from the offset ener-

gies. Experimental²⁵ and theoretical²⁶ studies of donor species in quantum wells have shown that the $1s - 2p_+$ energy increases relative to bulk GaAs, whereas all our offsets are less than this (Fig. 5, compared to a $1s - 2p_+$ energy of 4 meV for bulk). The remaining possibility is that the carriers are bound by monolayer-width fluctuations. The carriers localize in regions of the quantum well where the well is widest and hence the confinement energy is lowest. An offset can arise if the spatial extent of the step (in the layer plane) is larger than the cyclotron radius of the $n = 0$ level. The point is that the cyclotron radius of the $n = 1$ level is larger than the cyclotron radius of the $n = 0$ level and so the $n = 1$ energy is not perturbed as much as the $n = 0$ energy (it averages over a wider area). Hence an offset in the cyclotron-resonance energy appears. A strong well width dependence arises because a monolayer-width fluctuation changes the confinement energy more for a narrow well than for a wide well. This is precisely the trend in Fig. 5, where the offset increases rapidly with decreasing well width.

The cyclotron-resonance data were analyzed using Eq. (7) rather than Eq. (8), as it is not clear how a monolayer fluctuation can be modeled with a parabolic potential. The offset will be at most

$$\frac{d\varepsilon}{dL}\delta L, \quad (9)$$

where $\delta L \simeq 3$ Å, which assumes that only the $n = 0$ level is perturbed. This will not be the case in practice, and the offset will be smaller than this because the energy of the $n = 1$ level will also be pulled down, but to a lesser extent. Plotted in Fig. 5 is

$$\delta = \gamma \frac{d\varepsilon}{dL}\delta L, \quad (10)$$

with $\gamma \sim \frac{1}{3}$, and it can be seen to reproduce the data remarkably well.

For this picture to be accurate, the extent in the plane of the well width step d must be larger than the $n = 0$ cyclotron radius, otherwise the electrons would average out the perturbation in the course of their orbits. Also, d cannot be much larger than the $n = 1$ cyclotron radius, otherwise the offset would not appear at all. The lowest field we used was ~ 2 T, which implies roughly that $200 \leq d \leq 1000$ Å.

VI. CONCLUSIONS

Optically detected cyclotron resonance has been performed on a series of undoped GaAs quantum wells. The results show the following.

- (1) The band edge mass for in-plane motion can be related to the confinement energy with the theory of Ekenberg,⁵ based on $\mathbf{k} \cdot \mathbf{p}$ theory. It is important to include the nonparabolicity from both Γ_1^c - Γ_5^c and

Γ_1^c - Γ_5^v interactions in the band structure of bulk GaAs.

- (2) The samples have monolayer-width fluctuations, extending over ~ 500 Å, which localize the carriers, giving rise to an offset energy in the cyclotron energy.

ACKNOWLEDGMENTS

This work was funded by the Science and Engineering Research Council of the United Kingdom. One of us (R.J.W.) would like to thank Christ Church, Oxford for financial support.

-
- ¹M. G. Wright, N. Ahmed, A. Koohian, K. Mitchell, G. R. Johnson, B. C. Cavenett, C. R. Pidgeon, C. R. Stanley, and A. H. Kean, *Semicond. Sci. Technol.* **5**, 438 (1990).
- ²A. Moll, C. Wetzel, B. K. Meyer, P. Omling, and F. Scholz, *Phys. Rev. B* **45**, 1504 (1992).
- ³R. Romestain and C. Weisbuch, *Phys. Rev. Lett.* **45**, 2067 (1980).
- ⁴N. Ahmed, I. R. Agool, M. G. Wright, K. Mitchell, A. Koohian, S. J. A. Adams, C. R. Pidgeon, B. C. Cavenett, C. R. Stanley, and A. H. Kean, *Semicond. Sci. Technol.* **7**, 357 (1992).
- ⁵U. Ekenberg, *Phys. Rev. B* **40**, 7714 (1989).
- ⁶J. W. Orton, P. F. Fewster, J. P. Gowers, P. Dawson, K. J. Moore, P. J. Dobson, C. J. Curling, C. T. Foxon, K. Woodbridge, G. Duggan, and H. I. Ralph, *Semicond. Sci. Technol.* **2**, 597 (1987).
- ⁷D. C. Rogers, J. Singleton, R. J. Nicholas, C. T. Foxon, and K. Woodbridge, *Phys. Rev. B* **34**, 4002 (1986).
- ⁸A. S. Plaut, J. Singleton, R. J. Nicholas, R. T. Harley, S. R. Andrews, and C. T. B. Foxon, *Phys. Rev. B* **38**, 1323 (1988).
- ⁹J. Singleton, R. J. Nicholas, D. C. Rogers, and C. T. B. Foxon, *Surf. Sci.* **196**, 429 (1988).
- ¹⁰U. Rössler, *Solid State Commun.* **49**, 943 (1984).
- ¹¹F. Malcher, G. Lommer, and U. Rössler, *Superlatt. Microstruct.* **2**, 267 (1986).
- ¹²K. J. Moore, P. Dawson, and C. T. Foxon, *Phys. Rev. B* **34**, 6022 (1986).
- ¹³F. M. Peeters and J. T. Devreese, *Phys. Rev. B* **31**, 3689 (1985).
- ¹⁴M. A. Hopkins, R. J. Nicholas, P. Pfeffer, W. Zawadzki, D. Gauthier, J. C. Portal, and M. A. DiForte-Poisson, *Semicond. Sci. Technol.* **2**, 568 (1987).
- ¹⁵Hopkins *et al.* (Ref. 14) measure the band edge mass of bulk GaAs to be 0.0660, whereas Ekenberg takes 0.0665 (Ref. 5). For consistency with Ekenberg's theory, both curves in Fig. 6 use 0.0665.
- ¹⁶M. A. Hopkins, R. J. Nicholas, M. A. Brummell, J. J. Harris, and C. T. Foxon, *Phys. Rev.* **36**, 4789 (1987).
- ¹⁷E. O. Kane, *J. Phys. Chem. Solids* **1**, 249 (1957).
- ¹⁸G. Bastard, *Phys. Rev. B* **24**, 5693 (1981); **25**, 7584 (1982).
- ¹⁹H. Sigg, D. Weiss, and K. v. Klitzing, *Surf. Sci.* **196**, 293 (1988).
- ²⁰G. Wiggins, R. J. Nicholas, J. J. Harris, and C. T. Foxon, *Surf. Sci.* **229**, 488 (1990).
- ²¹J. Richter, H. Sigg, K. v. Klitzing, and K. Ploog, *Phys. Rev. B* **39**, 6268 (1989).
- ²²R. J. Nicholas, M. A. Hopkins, D. J. Barnes, M. A. Brummell, H. Sigg, D. Heitmann, K. Ensslin, J. J. Harris, C. T. Foxon, and G. Weimann, *Phys. Rev. B* **39**, 10955 (1989).
- ²³R. J. Warburton, R. J. Nicholas, L. K. Howard, and M. T. Emeny, *Phys. Rev. B* **43**, 14 124 (1991).
- ²⁴J. P. Kotthaus, G. Abstreiter, J. F. Koch, and R. Ranvaud, *Phys. Rev. Lett.* **34**, 151 (1975).
- ²⁵N. C. Jarosik, B. D. McCombe, B. V. Shanabrook, J. Comas, J. Ralston, and G. Wicks, *Phys. Rev. Lett.* **54**, 1283 (1985).
- ²⁶R. L. Greene and K. K. Bajaj, *Phys. Rev. B* **31**, 913 (1985).